# Influence of anaesthetics on the melting transition of lipid membranes

Benedicte Mengel      Maria Christiansen

31. May 2005

Bachelor Project
Membrane Biophysics and Thermodynamics Group
Niels Bohr Institute
University of Copenhagen
Supervisor: Thomas Heimburg

## Abstract

The mechanism by which anaesthetics work is much discussed. The most prevalent view is that anaesthetics bind to ligand gated ion channels thereby restricting their function. Another view is that anaesthetics interact directly with the cell membrane, changing properties of the membrane leading to a conformational change in the membrane proteins which causes anaesthesia.

In this thesis we will investigate the influence of general anaesthetics on the melting transition of artificial lipid membranes. This is done by calorimetry, pressure calorimetry and densitometry.

We find that the melting transition broadens and the melting temperature is lowered when anaesthetics are added, and pressure shifts the melting point to a higher temperature. Furthermore the relation between volume change and enthalpy change is found.

Anne Benedicte Mengel
cpr.nr. 240383-1614

Maria Christiansen
cpr.nr. 070682-2224

# Contents

# 1  Introduction

To outline the basis for our thesis, we will introduce the cell, lipid membranes, and anaesthetics. Further on we will give the motivation for studying the effect of anaesthetics on membranes.

## 1.1  The Cell

The cell is the basic unit from which living organisms are made. There is a vast number of different cell types, but the fundamental composition of all cells is the same: They consist of an aqueous solution of organic molecules enclosed by a lipid membrane, the plasma membrane. Procaryotes are essentially made of nothing more and live their lives as single-celled organisms. Eucaryotic cells on the other hand contain membrane bounded compartments such as the nucleus, the endoplasmic reticulum, the Golgi apparatus, mitochondria, and different kinds of vesicles, and they most often live in multicellular assemblies.

## 1.2  Lipid membranes

Lipids are amphiphilic molecules composed of a polar hydrophilic head group and nonpolar hydrophobic fatty acid tails (see fig. 1).
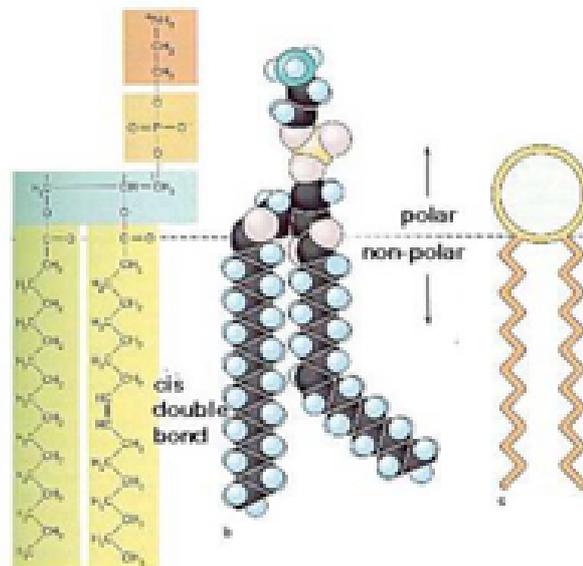


Figure 1: *Lipid molecule [1]*

Because of their amphiphilic character, lipid molecules spontaneously form aggregates when exposed to an aqueous environment. They can accumulate in several different structures, e.g. micelles, bilayers and inverse hexagonal phases (see fig. 2)
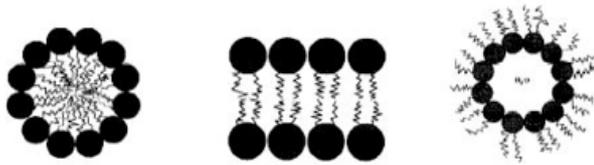
Figure 2: *Different structures of lipid aggregates. Left: Micelle. Middle: Bilayer. Right: Inverse hexagonal phase. [1]*

The most important of these structures is the lipid bilayer because all biological membranes consist of such a bilayer. It is approximately 5 nm thick, and containins different kinds of lipids and associated proteins. According to the fluid mosaic model the proteins are considered to be randomly distributed and to freely diffuse laterally within the bilayer [2]. Some membrane proteins act as highly selective channels allowing substances to go into or out of the cell, while others act as sensors that enable the cell to communicate with its surroundings. Different cell types have different membrane compositions of lipids and proteins, giving each of them specific abilities. The same is valid for the membrane bounded organelles in the cell.

In this thesis, all experiments, except for an AFM scan (sec. 3.1.3), were done with artificial lipid bilayers made-up by only one kind of lipid, DPPC (1,2-dipalmitoyl-sn-glycero-3-phosphocholine, see fig. 3), in order to keep the system as simple as possible. DPPC has two hydrocarbon chains each containing 16 carbon.
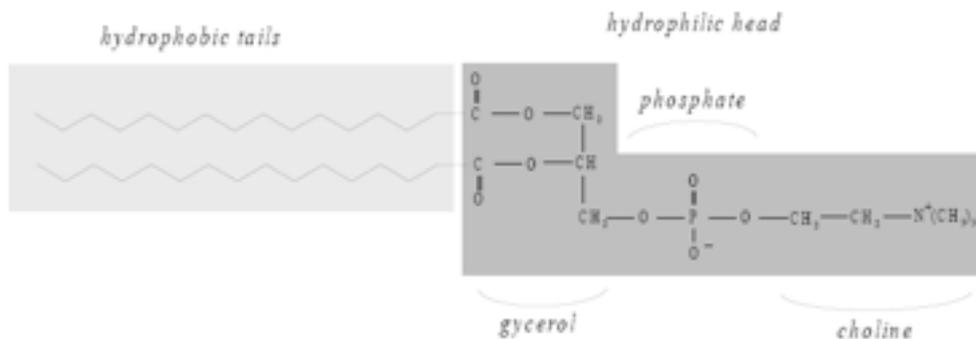


Figure 3: *Structure of DPPC [3]*

As seen in fig. 3, the hydrocarbon tails of DPPC are saturated, that is they do not contain any double bonds. Hence rotation around every C-C bond is possible. When a lipid membrane made of DPPC is in its state of minimum energy, the hydrocarbon chains of the lipids are all parallel and fully extended. This means that there is no rotation around the double bonds, the lipids are arranged in a lattice, and the structure of the membrane is crystalline. At room temperature the membrane is in a solid ordered state where the lipids are still arranged in

a lattice, but the chains are tilted, even though they still are parallel and fully extended.

When temperature increases, the energy and the entropy S of the system increases, and more states become accessible for the chains due to statistical principles. That is rotation around the C-C bond become more probable and the chain is disordered. When the lipids in a membrane are disordered and the lattice structure is broken, the state of the membrane is called liquid disordered, see fig. 4. Because the chains are kinked, the membrane gets thinner, and the lipids cannot pack as tight, which results in an area increase.
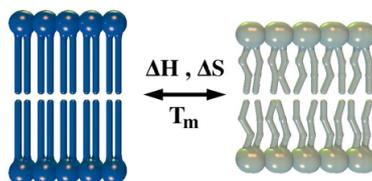


Figure 4: *Difference between solid ordered and liquid disordered membranes. When the membrane melts, the entropy, S, and the enthalpy, H, increases. $T_m$ is the melting temperature of the membrane. [4]*

In addition to the solid ordered and the liquid disordered state there is another state called the "ripple phase". In this phase the membrane has "ripples" due to line defects caused by disordered lipids facing ordered lipids [5]. The transition from the solid ordered (or gel) state to the "ripple phase" is called the pre-transition, and the transition from the "ripple phase" to the liquid disordered state is called the main transition. A heat capacity profile of DPPC containing the two transitions is shown in fig. 5.



Figure 5: *Heat capacity profile for DPPC*

The melting temperature $T_m$ of the lipid membrane is defined as the temperature at which 50 % of the lipids are ordered and 50 % are disordered.

The main transition is a cooperative process, which means that the melting of one lipid influences the melting of its neig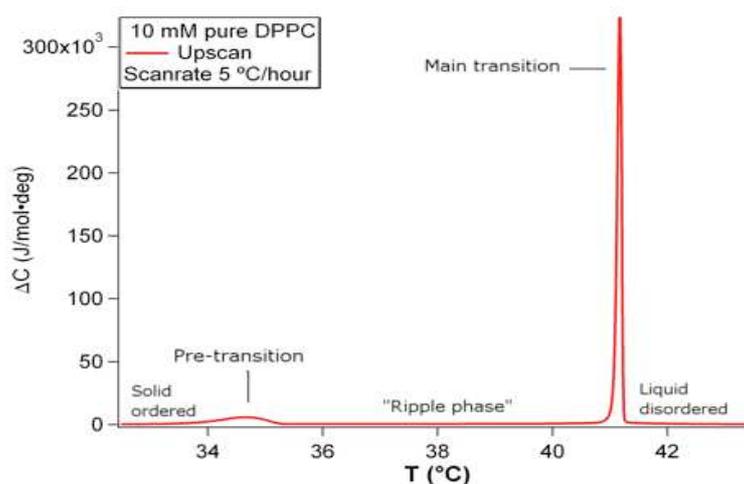hbours. A high cooperativity will make the peak of the main transition sharp because all lipids melt at approximately the same time.

### 1.2.1 Domains

During the main transition the lipids gradually melt. As disordered lipids are shorter than ordered, the upper part of the hydrophobic chains of the ordered lipids will be exposed to surrounding water if next to disordered lipids. In order to minimize the energy of the system, the ordered lipids will gather in domains. The domain size depends on the cooperativity of the transition [6]. If there is no cooperativity, the tension in the interface between ordered and disordered domains is zero. When there is no interfacial tension, ordered and disordered lipids will be randomly distributed. If the cooperativity on the other hand is high, it is energetically favourable for the lipids to form two domains, one containing ordered lipids only and the other containing disordered lipids only.

A Monte Carlo simulation of interactions between ordered and disordered lipids is compared to heat capacity profiles ([6]). In the simulation, several parameters can be varied in order for the simulation to resemble the heat capacity profile. One of the parameters is the interaction between ordered and disordered lipids. Fig. 6 to 8 (friendly provided by H. Seeger, Membrane Group, NBI) shows a simulation with three different values of the interaction parameter. In fig. 6 the parameter is the value at which the agreement between simulation and experimental data is best. The parameter has the order of magnitude $\frac{1}{2}k_BT$. In fig. 7 and 8 the parameter is changed to 90 % and 80 % of this value, respectively.
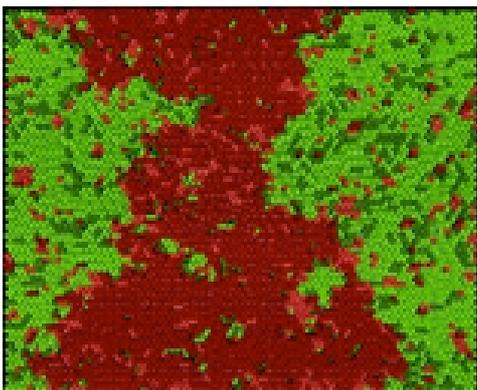


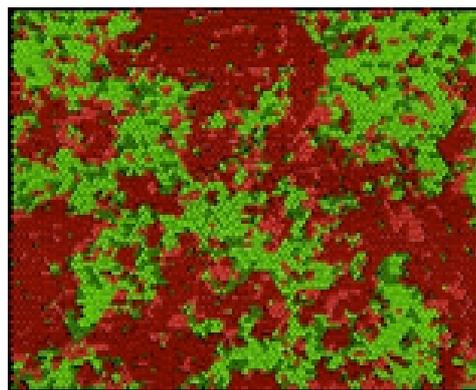Figure 6: *Monte Carlo simulation. Gel-fluid interaction parameter = 100 %. DMPC:DSPC = 50:50 at 310 K.*

Figure 7: *Monte Carlo simulation. Gel-fluid interaction parameter = 90 %. DMPC:DSPC = 50:50 at 310 K.*
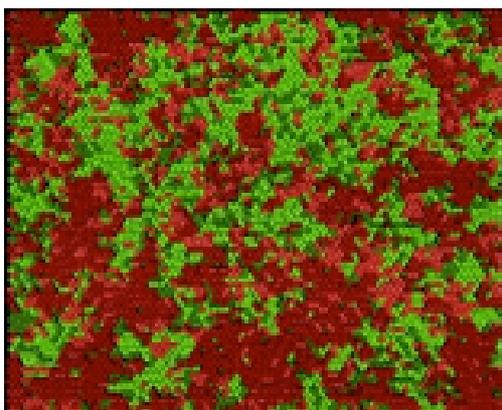
Figure 8: *Monte Carlo simulation. Gel-fluid interaction parameter = 80 %. DMPC:DSPC = 50:50 at 310 K.*

The simulation shows how the domain size depends on the interaction parameter. If the parameter is 100 %, large domains are formed, and if the parameter is lower, the domain size decreases. A decrease in domain size will lead to a broadening of the melting transition because of the diminished cooperativity.

## 1.3 Anaesthetics

Anaesthetics were introduced into clinical practice more than 150 years ago, but even though a lot of research has been done in this area, the molecular mechanisms of anaesthetics still remain obscure. During the last century the prevalent view of the mechanisms was that anaesthetics get incorporated in the membrane, thereby altering the conformational equilibrium of membrane proteins. This theory is based on the Meyer-Overton rule. Meyer [7] and Overton [8] independently stated that the anaesthetic potency of a substance is almost linearly correlated with its solubility in olive oil. This indicates that anaesthetics act on lipophilic sites.

In the last decades, deviations from the Meyer-Overton rule has been observed: 1) The potency of short- and long-chained alcohols ($n = 1$ and $n \geq 12$) is not as predicted, and 2) the potencies of enantiomers [1] are not the same. The breaking of the Meyer-Overton rule is of many considered a proof that anaesthetics bind to hydrophobic sites in membrane proteins and not the membrane itself ([9]-[11]), but Cantor gives an explanation of the deviations ([12]) which support the old theory.

At the moment, there are then two competing theories. One states that anaesthetics bind directly to membrane proteins, altering their conformation and thereby their functions ([9]-[11]). The nother states that the conformational changes of the proteins stem from changes in the membrane properties, caused by incorporation of anaesthetics in the membrane ([12]-[16]).

_____

[1]Enantiomers are two stereoisomers of which one can be superimposed on the mirror image of the other.

Many different substances can act as general anaesthetics. There is no characteristic structure, but the substances can be divided into four classes: 1) Volatile anaesthetics, 2) anaesthetic gases, 3) intravenous anaesthetics, and 4) alcohols (see fig. 9).
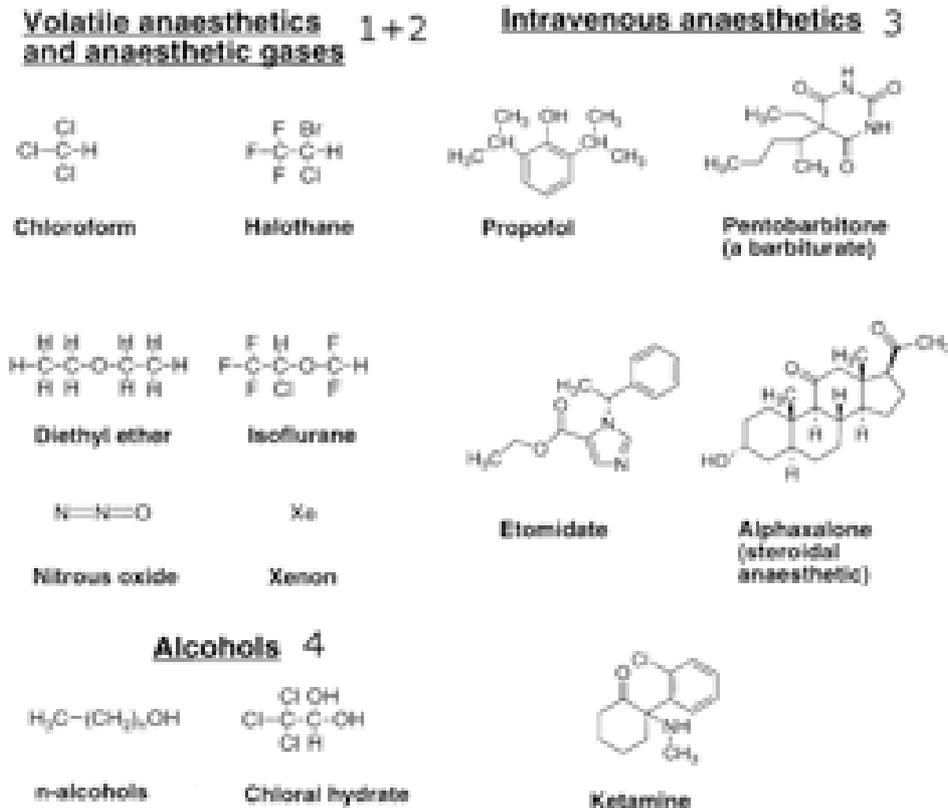


Figure 9: *The four classes of general anaesthetics [11]*

Furthermore, general anaesthetics can be recognized by providing several of the following effects on the body: Immobility, unconsciousness/hypnosis, amnesia, analgesia, muscle relaxation, and depression of autonomic reflexes.

Experiments in this project were done with 3 different kinds of anaesthetics: Octanol ($C_8H_{18}O$), halothane ($C_2HBrClF_3$) and dietylether (($C_2H_5)_2O$). Octanol has a clinically relevant concentration of 48 $\mu$M, diethylether of 10500 $\mu$M, and halothane of 200 $\mu$M [11].

## 1.4 Motivation

The melting transition of many membranes in biological systems lies just below body temperature. This is clever because many characteristic features change in the transition, and it is not so difficult to get into the melting transition when it

lies close to body temperature. For example it is shown in [17] that by lowering the pH in E. Coli it is possible to make the growth temperature and the transition temperature coincide.

We will examine whether anaesthetics might shift the melting transition of artifical membranes to a lower temperature. In biological systems this would mean that the transition is moved away from body temperature, thereby preventing the membranes to go into the transition, which could reduce essential processes.

On the basis of our examinations we will discuss if anaesthetics act directly on the membrane.

# 2 Theory

In this section we will introduce a thermodynamical view of the phase transitions introduced in section 1.2. Furthermore we will look at the proportionality between change in volume and change in enthalpy, $\gamma$, which can be found in two ways; either by comparing volume changes and changes in enthalpy during the phase transition or by comparing changes in temperature when pressure is applied.

## 2.1 Thermodynamical background to the phase transition

From basic thermodynamics [18] the expressions for Gibbs free energy and the enthalpy are known:
The Gibbs free energy is defined as

$$G = H - TS$$

and the enthalpy is

$$H = U + pV \tag{1}$$

where U is the internal energy, T the temperature, S the entropy, p the pressure, and V the volume.
The heat capacity of a system at constant pressure is

$$C_p = \frac{dQ}{dT}$$

The change in enthalpy is:

$$
\begin{aligned}
dH &= dU + d(pV) \\
&= T\,dS - p\,dV + p\,dV + V\,dp \\
&= T\,dS + V\,dp
\end{aligned}
$$

$dQ = T\,dS$ and we work at constant pressure ($dp = 0$), so the change in enthalpy with respect to temperature is:

$$\left(\frac{\partial H}{\partial T}\right)_p = \frac{dQ}{dT} = C_p \tag{2}$$

From eq. (2) it is possible to calculate the change in enthalpy:

$$\Delta H = \int_T^{T+\Delta T} C_p \, dT \tag{3}$$

If we consider an ensemble of lipids in state i, then the thermal average of a given value X is ([18])

$$\langle X \rangle = \frac{\sum X_i \exp(\frac{-\Delta H_i}{k_B T})}{\sum \exp(\frac{-\Delta H_i}{k_B T})}$$

where i is the number of possible states and $\sum \exp(\frac{-\Delta H_i}{k_B T}) = Z$ is the partition function.

The mean value of the change in enthalpy is then

$$\langle \Delta H \rangle = \frac{\sum \Delta H_i \exp(\frac{-\Delta H_i}{k_B T})}{\sum \exp(\frac{-\Delta H_i}{k_B T})} \tag{4}$$

By differentiating eq. (4) the excess heat capacity is obtained (see eq. (2)):

$$
\begin{aligned}
\frac{\partial \langle \Delta H \rangle}{\partial T} &= \frac{\sum \frac{\partial \Delta H_i}{\partial T} \exp\left(\frac{-\Delta H_i}{k_B T}\right)}{\sum \exp\left(\frac{-\Delta H_i}{k_B T}\right)} + \frac{\sum \Delta H_i \exp\left(\frac{-\Delta H_i}{k_B T}\right) \Delta H_i}{\sum \exp\left(\frac{-\Delta H_i}{k_B T}\right) k_B T^2} \\
&+ \frac{-\left[\sum \Delta H_i \exp\left(\frac{-\Delta H_i}{k_B T}\right)\right]^2}{\left[\sum \exp\left(\frac{-\Delta H_i}{k_B T}\right)\right]^2 k_B T^2} \\
&= \frac{\langle \Delta H^2 \rangle - \langle \Delta H \rangle^2}{k_B T^2}
\end{aligned} \tag{5}
$$

where the first term after the equality sign disappears because $\Delta H_i$ is constant.

Hence

$$\Delta C_p = \frac{\langle \Delta H^2 \rangle - \langle \Delta H \rangle^2}{k_B T^2} \tag{6}$$

9

This shows that the measured excess heat capacity relates to the enthalpy fluctuations in the system.

The mean value of the volume change is

$$\langle \Delta V \rangle = \frac{\sum_i \Delta V_i \exp(\frac{-\Delta H_i}{k_B T})}{\sum_i \exp(\frac{-\Delta H_i}{k_B T})}. \tag{7}$$

By inserting

$$\Delta H_i = \Delta U_i + p \Delta V_i$$

and differentiating with respect to temperature we obtain

$$\frac{\partial \langle \Delta V \rangle}{\partial p} = \frac{-\langle \Delta V^2 \rangle + \langle \Delta V \rangle^2}{k_B T} \tag{8}$$

The change in compressibility $\Delta K_T$ is defined as [19]:

$$\Delta K_T = -\frac{1}{\langle \Delta V \rangle} \left( \frac{\partial \Delta V}{\partial p} \right)_T = \frac{\langle \Delta V^2 \rangle - \langle \Delta V \rangle^2}{\langle \Delta V \rangle k_B T} \tag{9}$$

Here we see that the change in compressibility is proportional to fluctuations in volume.

## 2.2 The proportional factor $\gamma$

It is shown [19] that the change in volume is proportional to the change in enthalpy by a factor $\gamma$

$$\frac{d(\Delta V)}{dT} = \gamma \cdot \Delta C_p \longrightarrow \Delta V(T) = \gamma \cdot \Delta H(T), \tag{10}$$

This is not a theoretical finding but stems from experiments.

By inserting eq. (10) and eq. (6) in eq. (9) we obtain the relation between the change in compressibility and the excess heat capacity:

$$\begin{aligned} \Delta K_T &= \frac{\langle \Delta V^2 \rangle - \langle \Delta V \rangle^2}{\langle \Delta V \rangle k_B T} = \frac{T \langle \gamma^2 \Delta H^2 \rangle - \langle \gamma \Delta H \rangle^2}{\langle \Delta V \rangle k_B T^2} \\ &= \frac{T \gamma^2 (\langle \Delta H^2 \rangle - \langle \Delta H \rangle^2)}{\langle \Delta V \rangle k_B T^2} = \frac{\gamma^2 T}{\langle \Delta V \rangle} \cdot \Delta C_p . \end{aligned} \tag{11}$$

That is $\Delta K_T$ is proportional to the excess heat capacity.

In sec. 4.3 we investigate whether this proportionality also applies when anaesthetics are added, that is if $\gamma$ is the same with and without anaesthetics in the lipid bilayers.

$\gamma$ can be found in two ways, either by comparing the changes in enthalpy and volume (eq. (10)) or by comparing the melting temperature of the lipids at different pressures.

**Relation between temperatures at different pressures**
The change in enthalpy is given by

$$\Delta H_i = \Delta U_i + p_0 \cdot \Delta V_i$$

from eq. (1).
At a different pressure $(p_0 + \Delta p)$ the enthalpy change is given by

$$\Delta H_i^{\Delta p} = \Delta U_i + (p_0 + \Delta p) \cdot \Delta V_i \tag{12}$$

By inserting eq. (10) in eq. (12) we obtain

$$\Delta H_i^{\Delta p} = \Delta U_i + p_0 \cdot \Delta V_i + \gamma \Delta p \cdot \Delta H_i = \Delta H_i \cdot (1 + \gamma \cdot \Delta p) \tag{13}$$

The mean enthalpy at pressure $(p_0 + \Delta p)$ is

$$
\begin{aligned}
\langle \Delta H \rangle_T^{\Delta p} &= (1 + \gamma \cdot \Delta p) \frac{\sum \Delta H_i \exp\left(\frac{-(1+\gamma \cdot \Delta p)\Delta H_i}{k_B T}\right)}{\sum \exp\left(\frac{-(1+\gamma \cdot \Delta p)\Delta H_i}{k_B T}\right)} \\
&= (1 + \gamma \cdot \Delta p) \frac{\sum \Delta H_i \exp\left(\frac{-\Delta H_i}{k_B T^\star}\right)}{\sum \exp\left(\frac{-\Delta H_i}{k_B T^\star}\right)}.
\end{aligned}
\tag{14}
$$

That is (by eq. (4)):
$$\langle \Delta H \rangle_T^{\Delta p} \propto \langle \Delta H \rangle_{T^\star}^{p_0} \tag{15}$$

where $T^\star = \frac{T}{1+\gamma \cdot \Delta p}$ is the melting temperature at $p_0$, and T is the melting temperature at $(p_0 + \Delta p)$.

Hence it is possible to calculate $\gamma$ by comparing the melting temperatures and shape of the transitions at different pressures. The shape of the transitions should be identical if the assumption that $\Delta V = \gamma \cdot \Delta H$ is correct, because this assumption leads to eq. (15) which states that the area under the heat capacity profiles at different pressures is proprotional.

# 3 Materials and methods

In this section we will explain how the instruments we used work, and we will describe how the samples used in the different instruments were prepared. All of the samples were prepared by the same procedure, and the details are given in the following sections.

## 3.1 Sample preparation

### 3.1.1 Pure DPPC

The concentration of the lipids was calculated from the following equations:

$$c = \frac{n}{V} \tag{16}$$

and

$$n = \frac{m}{M} \tag{17}$$

where c denotes the concentration of the sample, n the moles, V the volume of the sample, m the mass of the lipids, and M the molar weight.

In all our experiments we used DPPC lipids with a molar mass of 734,05 g/mol from Avanti Polar Lipids (Alabaster/AL,USA) in the concentration 10 mM.

The lipid solutions were prepared in buffer (10 mM Hepes, 1 mM EDTA, pH 7,4). Buffer was used to ensure that the pH stayed the same during the whole experiment, because pH can alter the properties of the membrane. pH was buffered by Hepes, which buffers around pH 7. Furthermore buffer prevented any kind of growth of bacteria, because EDTA binds calcium which is essential for the growth of bacteria.

The mass of lipids needed to obtain a 10 mM solution was calculated from eq. (17) and (16) and weighed out within an error of $\pm$ 0.001 g, and buffer was added in the needed volume. The solution was then heated to above melting temperature $(T_m(DPPC) \approx 41°C)$ and stirred by a magnetic stirrer for 30 minutes, whereby multilamellar vesicles formed. Multilmellar vesicles are vesicles consisting of a stack of concentric spheres of lipid bilayers.

### 3.1.2 Anaesthetic

Anaesthetics were added as a weight percentage of the lipids, which were calculated in the following way:

$$\frac{m_{anaesthetic}}{m_{anaesthetic} + m_{DPPC}} = \frac{w\%}{100} \tag{18}$$

and added to the the lipid/buffer solution. If we for example wanted 1 ml 10 mM DPPC with 1 w% of anaesthetic, the calculation would be as follows:

$$\frac{m_{anaesthetic}}{m_{anaesthetic} + 1\ ml \cdot 10\ \frac{mmol}{L} \cdot 734.05\ \frac{g}{mol}} = 0.01$$

$m_{anaesthetic}$ is then isolated and divided by its molar mass in order to convert the mass to volume, because the anaesthetics we used are all liquids.

The volume of anaesthetic needed in our experiments was in the range of 0.1 $\mu$L which was too small a volume to measure out with our pipettes. Instead a reasonable volume of anaesthetic (3$\mu$L) was dissolved in buffer and a fraction of this solution was then dissolved in the lipid/buffer solution.

The first experiments with halothane were not reproducible. This could be due to the fact that halothane dissolves poorly in water, and it therefore is possible that halothane did not get into the membrane. With this in mind, we prepared the following samples with halothane by dissolving the halothane in methanol, a very water soluble alcohol, and adding a fraction of this to the lipid buffer solution. To see whether the methanol interacted with the membrane, an experiment was done with a sample only containing lipids and methanol in the same volume that we added in the experiments, $5\mu L$ in 2ml buffer. The result is shown in sec. 4.2.

Since octanol is water soluble, it was not necessary to add methanol to this part of the experiments.

### 3.1.3    Sample for Atomic Force Microscopy

Atomic Force Microscopy (AFM) was done at room temperature as it was not possible to control the temperature of the microscope. The sample used for AFM was a mixture of DPPC and DMPC (1,2-dimyristoyl-sn-glycero-3-phosphocholine) in the ratio 30:70. The heat capacity profile of this mixture is shown in fig. 10. (Friendly provided by J. Bruun, the Membrane Group, NBI.)
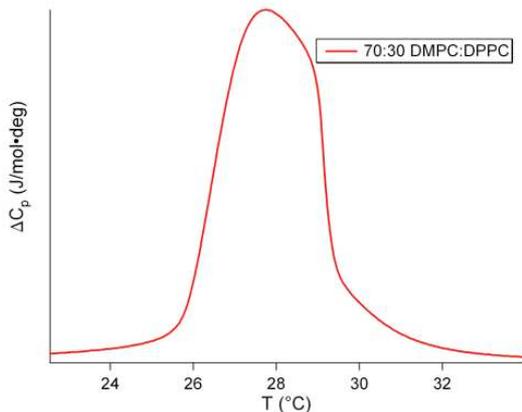


Figure 10: *Heat capacity profile of 70:30 DMPC:DPPC*

To mix the two lipids homogeneously they were dissolved in a solution containing dichloromethane and methanol in the ratio 2:1. The solution was then heated and the evaporating gases were blown away by a weak flow of nitrogen, whereby the solvent evaporated more quickly. To ensure the removal of all solvent molecules, the solution was desiccated over night. Two samples were made: One by adding buffer to the dried lipid mixture, and the other by adding both buffer and 1 w% octanol. When the lipids were completely dissolved in buffer, the samples were sonicated at 3 W for 10 minutes in intervals of 10 seconds with 10 seconds pauses in a Misonix 3000 sonicator to make vesicles with a diameter of approximately 20 nm. These so-called small unilamellar vesicles (SUV) have a very high surface tension due to their small diameter, and will therefore burst when they touch any

kind of surface. To keep the vesicles from fusing with each other, the samples were heated after sonication because liquid disordered membranes are less prone to fusing. In the AFM, mica was used as a support for the vesicles.



Figure 11: *The sample for AFM is placed on mica*

Mica is a mineral and it has a highly perfect basal cleaveage which makes the cleaved surface completely flat and clean. A small amount of solvent was placed on a disc of cleaved mica and left for 10-20 minutes in order for the vesicles to fuse on the mica (fig 11). Afterwards the sample on the disc was washed with a 1 mM NaCl solution and milli-Q water to wash away the surplus bilayers. It was important that the lipids on the mica were covered with water all the time, because the lipids, when exposed to air, would flip.

## 3.2 Instruments

### 3.2.1 Extruder

By extruding multilamellar vesicles it is possible to obtain unilamellar vesicles which only consist of one lipid bilayer. Unilamellar vesicles do not sink to the bottom of the solution like multilamellar vesicles, but stay in solvent, because of their small size and mass.

The extruder (Avestin Inc., Ottawa, Canada) consists of two syringes pushing the solvent through a polycarbonate filter with a pore size of 100 nm, see fig. 12.



Figure 12: *Extruder*

The extrusion had to be done at least 20 times both ways, to make sure that all the vesicles were unilamellar, and slowly so that the filter did not break. The extrusion was done above the melting temperature of the lipid membranes, because the membranes are then softer and easier to extrude. A sample of extruded vesicles is more transparent than a sample of multilamellar vesicles and has a hazy blueish colour.

### 3.2.2 Differential Densitometry

A differential densitometer measures the difference in densities of two liquids during heating. Each of the two samples of liquid was filled into a capillary in a cell (fig. 13) so that one cell (the sample cell) was filled with a lipid/buffer solution and the other cell (the reference cell) was filled with water. We should have used buffer as reference because the lipids were dissolved in buffer, but the densitometer was calibrated in respect to water, and therefore we used water as a reference instead of buffer.
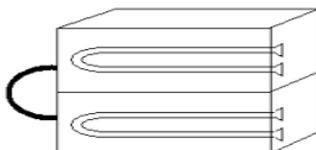


Figure 13: *Schematic drawing of the coupled cells in the densitometer.*

The cells are two coupled DMA 602M cells (Anton Paar, Graz, Austria). The reason for having coupled cells is that disturbances from the surroundings will be recorded by both cells, and since the densitometer measures the difference between the cells, the disturbances will not show up in the final data.

When the cells are filled, a computer controlled water bath starts heating the system, and the computer records the change in frequency of the vibration of the capillaries. When the density of the liquids decreases because of the volume expansion due to heating, the frequency of the vibration of the capillary will increase.

Before we put the liquid into the cells, it was degassed [2] to make sure that no air bubbles would form during the heating. The densitometer is a very sensitive instrument, and air bubbles therefore would perturb the results so that they are of no value. Furthermore, we used unilamellar vesicles because multilamellar vesicles were too heavy and would gather on the bottom of the capillary at the point where the oscillation had minimal amplitude. This would lead to an error in the measurement of the frequency of the capillary, since the weight distribution would become uneven.

**Handling the densitometry data**

As mentioned above, the densitometry measurements were made with lipids dissolved in buffer with water as reference. Because the lipids are dissolved in buffer, we ought to have made the measurements with buffer as reference instead of water. The difference in density between the two cells would then be the density of the lipids. The densitometer, however, was calibrated in respect to water and therefore it was not possible to use buffer as a reference. To compensate for the inaccuracy thereby obtained, we made a buffer/water measurement and subtracted it from the

---

[2]Degassing is done by putting the liquid under vacuum whereby air in the sample will gather in bubbles and seek to the surface of the sample where the pressure is lowest.

sample/water results, and in this way we obtained the same results as we would have had using buffer as reference.

The data from the densitometer was collected by the program LabView and analyzed by Igor Pro. The Igor program first converts the density to specific volume by the equation $V = \frac{M}{\rho_0}\left(1 - \frac{1000(\rho(T)-\rho_0)}{c}\right)$ [3] [21], and afterwards it differentiates the specific volume thereby obtaining the volume expansion coefficient $\frac{dV}{dT}$.

### 3.2.3 Differential Scanning Calorimetry

To analyze thermodynamical properties of lipid membranes, such as heat capacity and melting point, we used differential scanning calorimetry (DSC). We used a VP-DSC, produced by Microcal (Northhampton/MA, USA). It consists of two cells enclosed in an adiabatic box isolated from the surroundings (fig. 14).
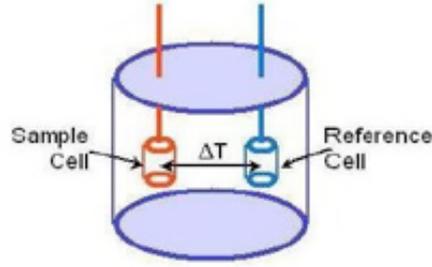


Figure 14: *Differential scanning Calorimeter*

One cell was filled with sample and the other with a reference solution, in our case buffer. The pressure in the calorimeter is approximately 50 psi = 4.4 bar when the lid is properly tightened. The calorimeter increases or decreases the temperature with a defined scan rate during the experiment, keeping the temperature difference between the two cells equal to zero. The difference in power needed to heat the two cells is called the excess power, $\Delta$P. By integrating the excess power with respect to time, the excess heat added to the sample is found to be:

$$\Delta Q = \int_t^{t+\Delta t} \Delta P(t')dt' \cong \Delta P \cdot \Delta t \qquad (19)$$

The heat capacity is given by the energy needed ($\Delta$Q) to heat the system $\Delta$T at constant pressure:

$$\Delta C_p = \left(\frac{\Delta Q}{\Delta T}\right)_p = \frac{\Delta P}{\left(\frac{\Delta T}{\Delta t}\right)} \;. \qquad (20)$$

where $\frac{\Delta T}{\Delta t}$ is the scan rate.

---

[3]M is the molar mass, $\rho$ is the density of the sample, $\rho_0$ is the density of the reference and c is the concentration of lipids in the sample in g/L

**Pressure Calorimetry**
A self-built pressure cell was added to the differential scanning calorimeter enabling us to alter the pressure on the lipids. The pressure cell is a small capillary with a volume of $\sim 60 \mu L$. Both calorimeter cells were filled with degassed distilled water to ensure a continuous flow of heat to the pressure cell. The pressure cell was lowered into the calorimeter. The calorimeter was closed by wrapping parafilm (Parafilm "M" Laboratory Film, Pechiney Plastic Packaging, Chicago) around the pressure cell and the opening in the calorimeter. This was done to avoid evaporation. The pressure cell was connected to a nitrogen gas container with a pressure reducer. It was possible to control the intake and release of nitrogen with several valves (Nova Swiss, Effretikon, Swizerland).

**Handling the calorimetry data**
The calorimeter is controlled by a computer. With the control program provided by MicroCal it is possible to set the scan temperature interval and the scan rate. It is important not too scan to fast because of the relaxation time of the membrane. If the scan rate is too high, the membrane will not reach equilibrium at one temperature before it is heated again.

Every experiment done consists of four scans:

1. 25 °C to 50 °C with a scan rate of 5 °C/hour

2. 50 °C to 25 °C with a scan rate of 5 °C/hour

3. 38 °C to 45 °C with a scan rate of 2 °C/hour

4. 25 °C to 50 °C with a scan rate of 5 °C/hour

The second scan is made to check if the process is reversible, see sec. 4.1, the third scan is done to look closer at the main transition, and the fourth scan is a backup of the first, because the lipids were not always completely dissolved when we started the experiment. One data point is produced every second, but to lower the sensitivity to minor disturbances, only the average of ten data points is recorded.

The data output is the heat capacity $C_p$ as a function of temperature T. We are only interested in the excess heat capacity in the transitions and not the heat capacity of the lipids in between the transitions. Everything but the excess heat capacity is therefore left out from the data by subtracting the baseline. This baseline is obtained by fitting a polynomial to the part of the curve not containing the two transitions (fig. 15). This is done in Igor Pro (a graphics program from WaveMetrics, Inc., version 4.0.7.0).

The enthalpy of the transitions is obtained by integrating the heat capacity in the relevant temperature interval, see eq. (3).

It can be hard to estimate how large an interval can be removed from the profile in order not to reduce the validity of the fit. We have in all of our data analysis left out as little data as possible.

There is an uncertainty in calculating the enthalpy as a result of the difficulties in defining the start and final temperature of the transitions.
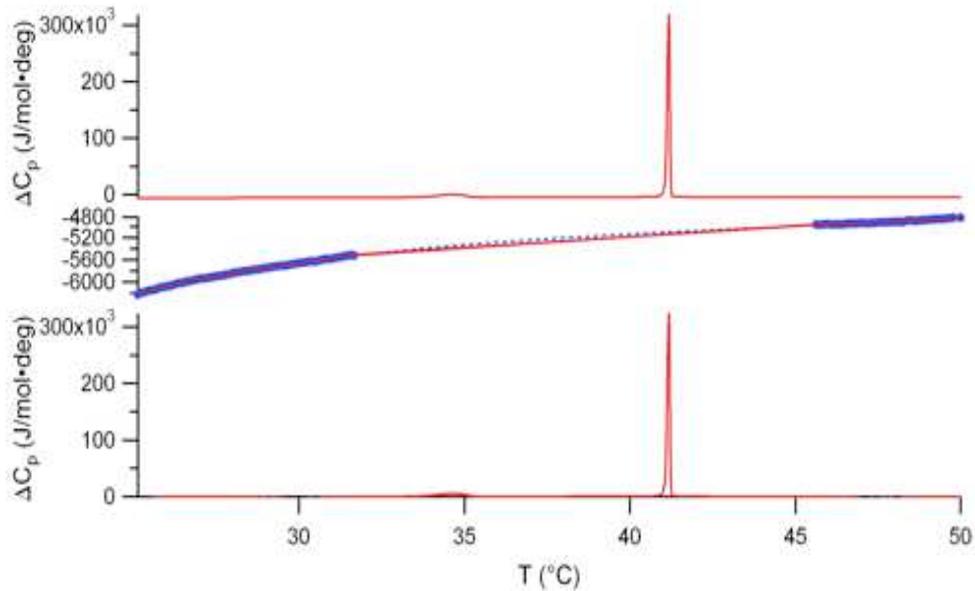
Figure 15: *Upper: Heat capacity profile without baseline correction. Middle: Baseline, that is the curve not containing the two transitions. Lower: Baseline corrected heat capacity profile.*

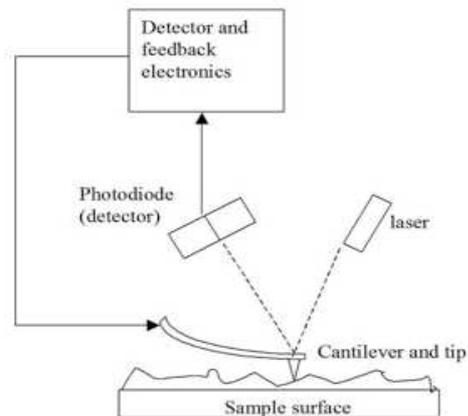### 3.2.4 Atomic Force Microscopy



Figure 16: *Atomic Force Microscope [20].*

An AFM scan is done by bringing the sharp tip of a cantilever into contact with the sample surface and moving the cantilever from side to side. The force between the sample and the tip leads to a deflection of the cantilever. A laser beam reflected from the top of the cantilever hits a detector which records the movement of the beam, fig. 16.

18

A height profile of the 70:30 DMPC:DPPC sample (sec. 3.1.3) is shown in fig. 17. The lightest areas, with a height of 20 nm, are parts of lipid bilayers that did not get washed of the mica during the sample preparation.
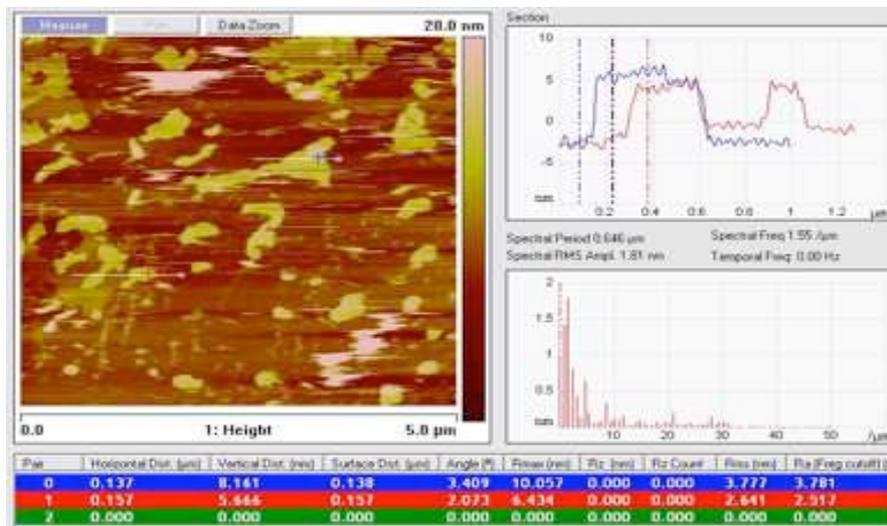


Figure 17: *Height profile from AFM*

The height profile of our sample is not as expected. The ligth areas are approximately 5 nm high, which corresponds to the thickness of a lipid bilayer. This indicates that our sample did not stand long enough for the vesicles to fuse on the mica. The light areas are then pieces of lipid bilayer, and the dark areas are mica.
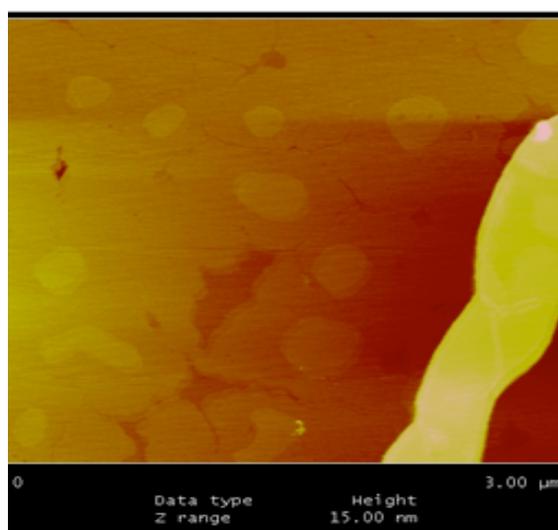


Figure 18: *Height profile from AFM*

Fig. 18 (friendly provided by V. Oliynik, Membrane Group, NBI) shows what

the scan would have looked like if the vesicles had time to fuse properly on the mica.

The small, light areas are domains of ordered lipids. These domains are approximately 0.5 nm higher than the surrounding domains, which is explained by the fact that disordered lipids have kinked chains and therefore are shorter.

# 4 Results

In the following sections we present the obtained results.

We have compared calorimeter experiments with different weight percents of the same anaesthetic to see any changes in transition properties caused by a change in concentration of anaesthetic. Furthermore we have compared experiments with 1 w% octanol at different pressures, and we have calculated $\gamma$ from the appropriate experiments.

## 4.1 Heat capacity profiles of pure DPPC

First of all we will look at an up scan compared to a down scan to see if the phase transition is reversible.
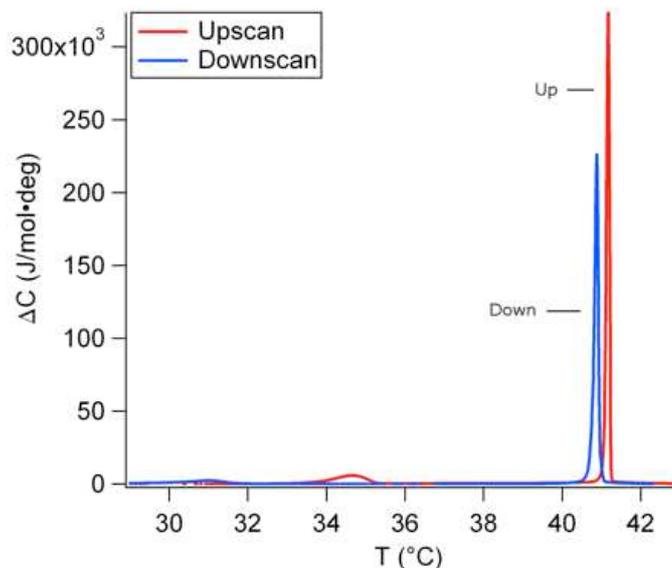


Figure 19: *Heat capacity profiles of up scan and down scan of pure DPPC*

Fig. 19 shows that the melting temperature of the down scan is lower than of the up scan. The difference is due to hysteresis, so if the scan rate had been infinitely low in both scans, the two graphs would have been identical. When the lipids are heated it takes a while for them to respond to the heat and the melting temperature is higher. Likewise when they are cooled. The graph shows that the

pre-transition takes place at a lower temperature in the down scan. This indicates that it takes longer time to form the "'ripple phase"' in the down scan.

On the basis of our considerations and the fact that the two curves have similar shapes, we conclude that the process is reversible.

## 4.2 Heat capacity profiles of DPPC with anaesthetics

### 4.2.1 Octanol

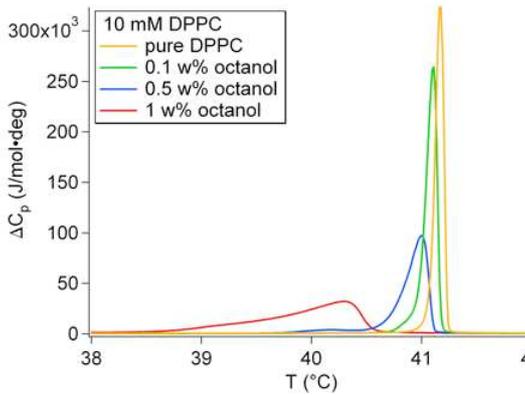Experiments were done with 0.1, 0.5 and 1 w% octanol.



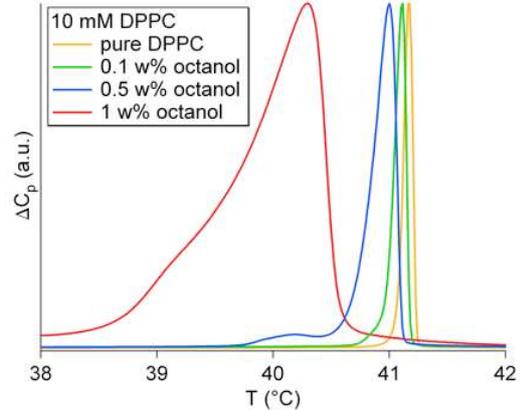Figure 20: *Heat capacity profiles of DPPC and octanol*

Figure 21: *Rescaled heat capacity profiles of DPPC and octanol*

a.u. stands for arbitrary units.

The profiles broaden and the melting temperature shifts downwards the more octanol is added. Furthermore the profiles becomes asymmetric. The broadening is caused by a decrease in domain size, sec. 1.2.1, that is the octanol decreases the interfacial tension between the solid ordered and liquid disordered state.

The asymmetry and the shift of the profiles is due to the fact that octanol favours the liquid phase. Octanol consists of a chain of eight carbon atoms and is much shorter than the membrane. As the disordered lipids are shorter than the ordered, the interfacial energy between ordered lipids and octanol is higher than between the disordered lipids and octanol. Therefore it is more energetically favourable for the membrane that the disordered lipids are in contact with octanol and the melting will start earlier. This also brings the melting temperature down.

When the transition is asymmetric, $T_m$ is no longer the temperature where the heat capacity is at its maximum, $T_{max}$. Technically $T_m$ is the temperature at which the the change in enthalpy is 50% of the entire enthalpy in the transition, but we have decided to use $T_{max}$ as an expression of $T_m$. This will lead to no wrong conclusion because $T_{max}$ will always be larger or equal to $T_m$.

The shoulder on the curve for 0.5 w% octanol seen in fig. 21 is most likely due to an inhomogeniety in the lipid solution.

In tab. 1 $T_{max}$ and the enthalpy changes in the main transition of DPPC with octanol are listed:

| Concentration (w %) | $T_{max}$ (°C) | $\Delta H$ (J/mole of lipids) |
|---|---|---|
| 0 | 41.15 | 33025 |
| 0.1 | 41.11 | 36120 |
| 0.5 | 41.00 | 36553 |
| 1.0 | 40.29 | 26670 |

Table 1: *Results of measurements with octanol*

The enthalpy changes are the same within the uncertainty in weighing out the lipids. The enthalpy change in the main transition of DPPC with 1 w% octanol is lower than the other values which can be due to an error in weighing out the lipids in this sample. The fact that the changes in enthalpy are the same shows that octanol does not influence the amount of energy needed to heat up one mole of lipids.

### 4.2.2 Halothane

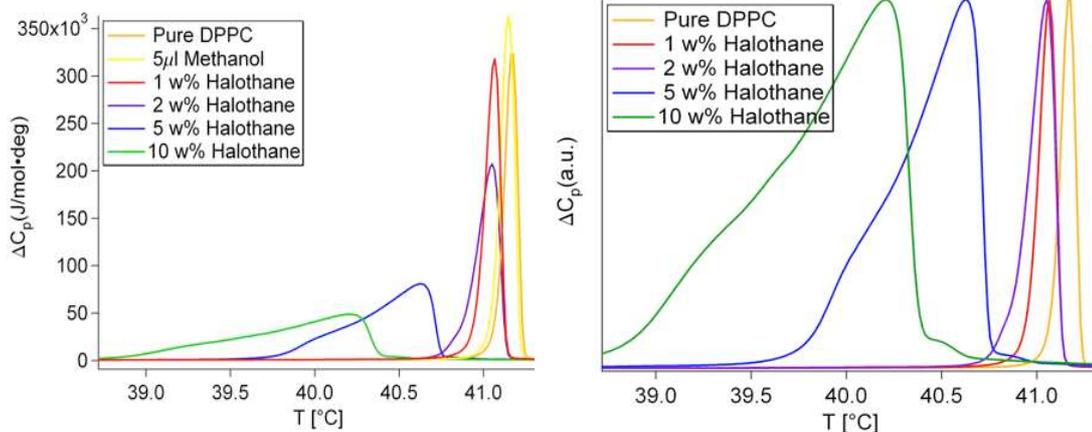The experiments with halothane was done with a concentration of 1, 2, 5 and 10 w%.



Figure 22: *Profile of DPPC with halothane*  Figure 23: *Rescaled profile of DPPC with halothane*

The melting temperatures shift downwards, the main transitions broaden and the profiles become asymmetric, as when octanol is added. We have plotted the curve for 2 ml 10 MM DPPC with 5 $\mu l$ methanol in fig. 22 to show how large an effect the methanol has on the lipid bilayers. We see that methanol has an effect, but it is so small that the effect of halothane alone is still considerable.

The enthalpy changes and $T_{max}$ are shown in tab. 2:

| Concentration (w %) | $T_{max}$ (°C) | $\Delta$ H (J/mole of lipids) |
|:---:|:---:|:---:|
| 0 | 41.15 | 33025 |
| 1 | 41.06 | 37015 |
| 2 | 40.93 | 37345 |
| 5 | 40.61 | 40979 |
| 10 | 40.20 | 38715 |

Table 2: *Results of measurements with Halothane*

The enthalpy changes are approximately the same, so halothane does - like octanol - not influence the amount of energy needed to heat up one mole of lipids.

We noticed that the curves of 1 w% octanol and 10 w% halothane have similar shapes and have maximum at approximately the same temperature. To examine the relationship of the two graphs we have plotted them together (fig. 24), and rescaled and shifted them (fig. 25) in order to get a better comparison.
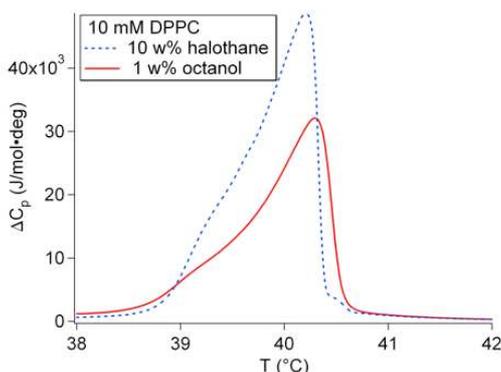


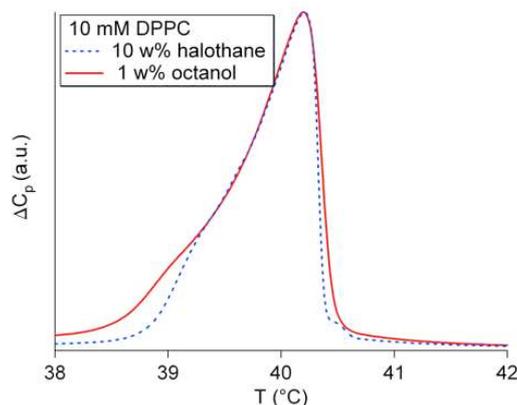Figure 24: *Profile of DPPC with 10 w% halothane and 1 w% octanol*



Figure 25: *Rescaled and shifted profile of 1 w% octanol and 10 w% halothane*

The shape of the two profiles is almost identical. This indicates that the domain size in the two cases is the same, which means that 1 w% octanol and 10 w% halothane decrease the interfacial tension between the phases of the lipids equally. The difference between $T_{max}$ of the two curves in fig. 24 is $40.30 - 40.21 \approx 0.1$°C.

10 w% halothane corresponds to 4030 $\mu M$ and 1 w% octanol corresponds to 569.6 $\mu M$. To obtain the same shift in melting temperature, we then need $\frac{4030\mu M}{569.6\mu M} \sim 7.1$ times higher concentration of halothane than octanol. It is worth noting that the ratio of the clinically relevant concentrations of halothane and octanol is 200 $\mu M$ : 48 $\mu M$ = 4 : 1 [11] (sec. 1.3).

To see if the relation was the same for 0.1 w% octanol and 1 w% halothane we plotted these graphs as well (fig. 26 and 27).
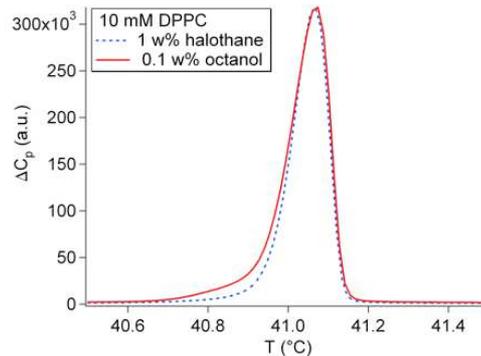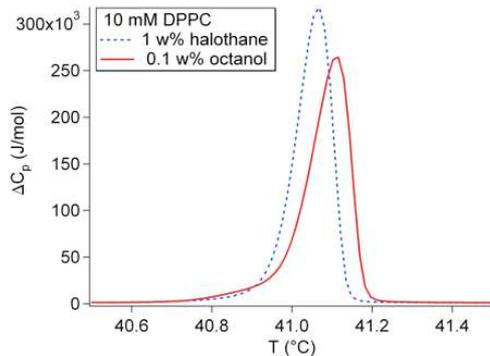
Figure 26: *Profile of DPPC with halothane and octanol*



Figure 27: *Rescaled and shifted profile of octanol and halothane*

As in fig. 25 the shape of the two profiles is almost identical. The difference in $T_{max}$ of the two curves is $41.11 - 41.07 = 0.04$ °C. 1 w% halothane corresponds to 375.6 $\mu M$ and 0.1 w% octanol corresponds to 56.4 $\mu M$, which are very close to the clinically relevant concentrations. The ratio between the needed concentrations of the two anaesthetics is $\frac{375.6 \mu M}{56.4 \mu M} \sim 6.7$.

The two comparisons indicate that approximately 7 times more halothane than octanol is needed to obtain a certain change in transition properties.

### 4.2.3 Diethylether

The heat capacity profiles of different concentrations of diethylether have nearly the same $T_m$ compared to each other, only differing with 0.01 °C, fig. 28. To make the difference between the profiles more visible, we have made a zoom of fig. 28 in fig. 29 because is looks as if there is only one curve in fig. 28. We have compared the results to data for pure DPPC. The graph of pure DPPC is narrower, and the melting temperature is 0.04 °C lower. A shift this tiny can be explained by a pressure difference in the calorimeter cells dependent of how much the lid was tightened.
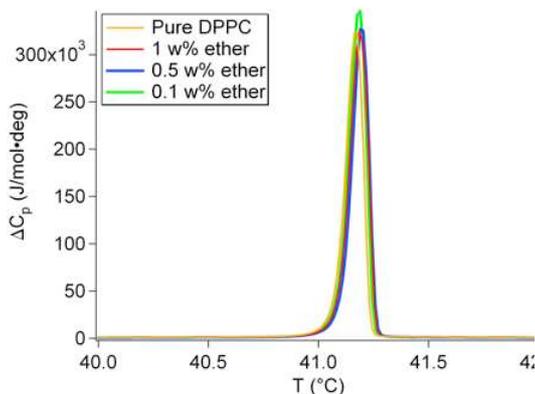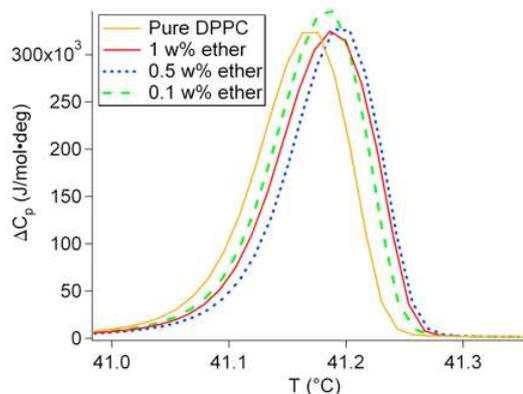


Figure 28: *Ether profile*



Figure 29: *Ether profile zoomed*

24

We did not expected to see no effects with anaesthetic in the membrane. This could be due to the fact that the concentration of ether in the lipids is different than we thought, either because 1) the concentration was too small, 2) it evaporated, or 3) it did not get incorporated in the membrane.

1) To obtain the same clinical effect with ether as with octanol, 200 times as much ether is needed. In the light of the comparison between 1 w% octanol and 10 w% halothane, we assume that there is a connection between the clinically relevant concentration and the effect on the melting transition of the membrane. Therefore it is reasonable to presume that we have not added enough ether to see an effect.

2) The boiling point of ether is 34,2 °C and the sample was heated to 50 °C several times during the preparation, so evaporation is also a reasonable explanation.

3) We assume that when the anaesthetic is dissolved in water it is also incorporated in the membrane. Diethylether was clearly dissolved, thus this is most likely not the problem.

Another reason why ether does not show any effect could be that it does not work as an anaesthetic by influencing the lipid membrane. This explanation is not probable, partly because the first two explanations above are very satisfactory and partly because of the uncertainty of our data.

### 4.2.4 Pressure calorimetry

Pressure experiments were done with 10 mM DPPC and 1 w% octanol at 1, 4.4, 90.2 and 160.4 bar. 1 bar is obtained by removing the lid from the calorimeter. Instead the opening is covered with parafilm to prevent impurities. 4.4 bar is the usual pressure in the cells when the lid is on, and higher pressure is obtained by using the pressure cell (sec. 3.2.3). Our results are shown in fig. 30 and 31.
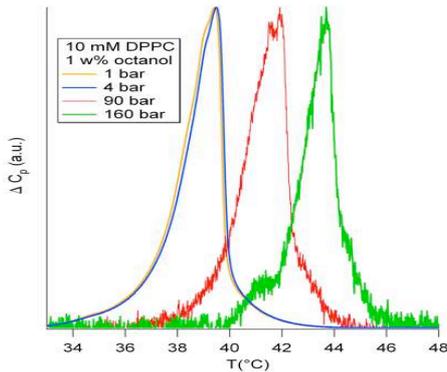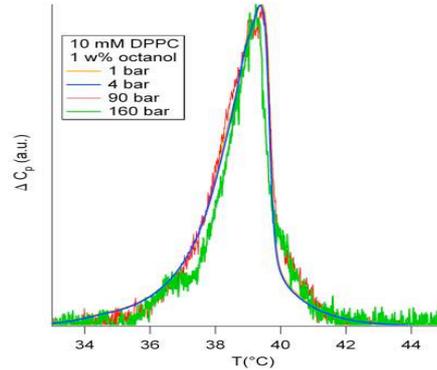


Figure 30: *Pressure profiles rescaled.*

Figure 31: *Pressure profiles and temperature axis rescaled.*

By looking at the rescaled pressure profiles in fig. 30 one can conclude that application of pressure on the membrane shifts the phase transition to a higher temperature. We find that a pressure change of 40 bar leads to a temperature shift of ∼1 °C. The same is found in [19].

The similar shape of the curves suggests that pressure does not change the cooperativity of the lipid bilayers which supports the assumption that $\Delta V = \gamma \Delta H$ (eq. (10)).

## 4.3 Calculation of $\gamma$

In this section we want to calculate the proportional factor $\gamma$ between change in volume and change in enthalpy (eq. (10)) for DPPC with and without anaesthetics to see if anaesthetics influence the change in compressibility during the phase transition.

As mentioned in sec. 2.2 it is possible to calculate $\gamma$ in two ways, either by comparing the changes in enthalpy and volume or by comparing the melting temperature of the lipids at different pressures. The pressure method is much more precise than the enthalpy/volume-comparison. This is due to the fact that we need to know the exact concentration of lipids in both the densitometer and the calorimeter to find the correct enthalpy and volume, whereas the pressure method uses the difference in pressure. By looking at the difference, the uncertainty in lipid concentration is eliminated.

**Calculation of $\gamma$ from comparison of change in volume and enthalpy**
In this section we want to find $\gamma$ by comparing change in volume and change in enthalpy (eq. (10)). The densitometry data $\frac{dV}{dT}$ is plotted in the same graph as the calorimetry data $\Delta C_p$ and the curves are superimposed.
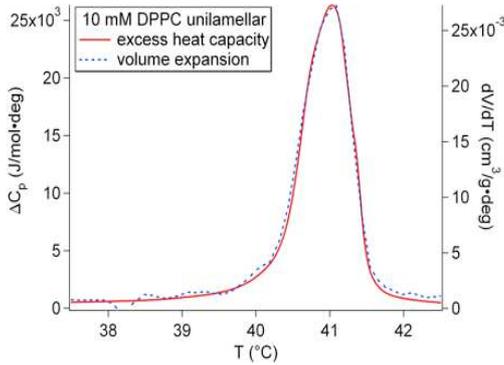


Figure 32: *Volume and enthalpy changes for pure DPPC.*
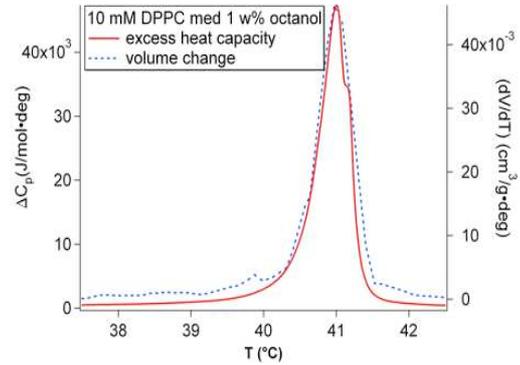
Figure 33: *Volume and enthalpy changes for DPPC and 1 w% octanol.*

We see in fig. 32 and 33 that the volume changes and the changes in heat capacity have very similar shapes when superimposed. Thus the assumption that $\Delta V = \gamma \Delta H$ is true.

It easier to find the height of the curves $(\frac{dV}{dT})_{max} - (\frac{dV}{dT})_{min}$ and $(\Delta C_p)_{max} - (\Delta C_p)_{min}$ at $T_m$ than to find $\Delta V$ and $\Delta H$. We are allowed to compare the heights of the curves instead of the areas below, because the relationship between the

heights is the same as between the areas as the curves have the same shape. The calculated values of $\gamma$ are shown in tab. 3.

| | Height of $\frac{dV}{dT}$ ($10^{-3}\frac{cm^3}{g\cdot deg}$) | Height of $\Delta C_p$ ($\frac{J}{mol\cdot deg}$) | $\gamma$ ($10^{-4}\frac{ml}{J}$) |
|---|---|---|---|
| Pure DPPC | $27.069 - 0.986 = 26.083$ | $26326.0 - 519.9 = 25806.11$ | 7.42 |
| 1 w% octanol | $44.844 - 0.716 = 44.128$ | $47342.0 - 1216.1 = 46125.90$ | 7.02 |

Table 3: $\gamma$ *obtained by comparing change in volume and enthalpy*

Octanol does not change the relationship $\gamma$ between volume and enthalpy changes within error. The mean value of $\gamma$ is $7.22 \cdot 10^{-4}\frac{ml}{J}$

In [19] $\gamma$ is found to be $\sim 8.14 \cdot 10^{-4}\, ml/J$ for DPPC (unilamellar vesicles).

**Calculation of $\gamma$ from pressure calorimetry**
From the data in the pressure graphs (fig. 30 and 31) it is possible to calculate the proportional factor $\gamma$ (tab. 4) by means of eq. (14).

| | $\Delta p$ (bar) | $\Delta T_{max}$ (°C) | $\gamma$ ($10^{-4}\frac{ml}{J}$) |
|---|---|---|---|
| 1 w% octanol | $4.4 - 1 = 3.4$ | $39.492 - 39.420 = 0.072$ | 6.59 |
| 1 w% octanol | $90.2 - 1 = 89.2$ | $41.717 - 39.420 = 2.297$ | 8.25 |
| 1 w% octanol | $160.4 - 1 = 159.4$ | $43.595 - 39.420 = 4.175$ | 8.39 |

Table 4: $\gamma$ *obtained from pressure calorimetry*

The mean value of $\gamma$ is $7.74 \cdot 10^{-4}\frac{ml}{J}$. In [19], $\gamma$ is found to be $\sim 7.5 \cdot 10^{-4}\, ml/J$ for DPPC (unilamellar vesicles).

The average value of $\gamma$ from all experiments is $7.53 \cdot 10^{-4}\frac{ml}{J}$.

The values of $\gamma$ found in the two experiments are the same within error. This means that the relation between the change in compressibility and excess heat capacity does not change when anaesthetics are added.

## 4.4   Errors

We have several error sources in the sample preparation. The weighing of the DPPC is uncertain with $\pm$ 0.0001 g, and the 2 ml pipettes are accurate within an error of 2 $\mu l$. Anaesthetics were added by two different methods, either by dissolving it in buffer or by dissolving it in methanol. When dissolving in buffer, the solubility of the anaesthetics is also of great importance. If the anaesthetic is not completely dissolved, the fraction of the buffer/anaesthetic- solution added to the lipids does not necessarily contain the expected amount of anaesthetic.

Because we manually define the temperature interval over which we integrate $\Delta C_p$, there is an uncertainty in $\Delta H$ in the different experiments.

The pressure in the calorimeter was not the same in every experiment, because the lid was not tightened equally much. The pressure was $50 \pm 1.5$ psi $= 3.4 \pm 0.1$ bar, and a pressure of 1.5 psi shifts the melting temperature by $\pm 0.0017$°C.

The lipids in the pressure cell are not all heated by the calorimeter because the pressure cell is too big to be lowered completely into the calorimeter cell. Because we do not know the exact amount of sample it is impossible to calculate the excess heat capacity.

# 5    Discussion and conclusion

The purpose of our thesis was to examine the influence of general anaesthetics on lipid membranes by means of differential scanning calorimetry, pressure calorimetry and differential densitometry. We used artificial membranes made of DPPC and added three different kinds of general anaesthetics, namely octanol, halothane and diethylether.

It is clear that octanol and halothane exert an effect on the melting transition of DPPC: The main transition broadens and becomes asymmetric, and the melting temperature is shifted to a lower temperature the more anaesthetic added. All of this can be due to a decrease in domain size which means that the interfacial tension between ordered and disordered lipids decreases.

The assumed change in domain size caused by anaesthetics can be connected with Cantor's theory about how small membrane soluble molecules can lead to a change in the lateral pressure profile of lipid bilayers, thereby modulating protein conformational equilibrium ([13], [14]). A possible explanation of how anaesthetics cause anaesthesia could then be that anaesthetics indirectly change the conformational equilibrium of membrane proteins. This change could alter the function of the proteins thereby leading to anaesthesia.

By comparing experiments with octanol and halothane we showed a connection between the amount of anaesthetic used and the obtained effect. 1 w% octanol corresponding to 569.6 $\mu M$ had the same effect as 10 w% halothane corresponding to 4030 $\mu M$, and 0.1 w% octanol corresponding to 56.4 $\mu M$ had the same effect as 1 w% halothane corresponding to 375.6 $\mu M$. This means that we need 7 times more halothane than octanol to shift the melting temperature by the same amount. The clinically relevant concentration of halothane is 4 times bigger than that of octanol [11]. This suggests that there is a close connection between the clinically relevant concentrations and the shift and change in shape of the melting transition yielded by anaesthetics, leading to the conclusion that anaesthetics act directly on membranes.

The concentrations of 1 w% halothane and 0.1 w% octanol are very close to the clinically relevant concentrations of the two anaesthetics. It is therefore reasonable to assume that clinically relevant concentrations of anaesthetics can have an influence on the membrane properties and thereby on membrane function.

The experiments with diethylether showed hardly any effect on the melting transition. On the basis of the discussion in sec. 4.2 we conclude that this is either due to evaporation or adding too little an amount of ether. It is not possible to decide which possibility is correct, but an experiment with a much larger concentration

of ether would decide this.

When lipid bilayers are put under pressure, the melting transition is shifted to a higher temperature, 0.97 °C every 40 bar ($T_m = (41.15 + 273.14)K \cdot (1 + 7.53 \cdot 10^{-4} ml/J \cdot 40 bar)$). Thus pressure shifts the melting transition to a higher temperature whereas anaesthetics shift the transition to a lower temperature. Pressure then cancel the effect of anaesthetics. This has been shown in experiments with rats that were first anaesthetized and afterwards put in a high-pressure chamber which removed the anaesthesia. [22]

The proportional factor $\gamma$ was calculated in two ways, sec. 2.2 and was found to be the same within error in both calculations. We also found that octanol did not change $\gamma$ which means that the relation between volume change and enthalpy change is constant.

The compressibility change $\Delta K_T$ is proportional to $\Delta C_p$ (eq. (9)). In the phase transition, $\Delta C_p$ increases and therefore $\Delta K_T$ increases. This means that the lipid bilayers become softer and fuse easier. When anaesthetics are added, $\Delta C_p$ is lowered, and as $\gamma$ is shown to be constant in the presence of anaesthetics, $\Delta K_T$ must also be lowered. This means that it is harder for the bilayers to fuse. Since much of the communication between cells is done by fusing vesicles containing transmitters with other membranes, anaesthetics might also have an effect by inhibiting this kind of communication between the cells.

After taking all of the above arguments into consideration, we conclude that there are indications that some anaesthetics act directly on the membrane, changing the membrane function. We cannot exclude that anaesthetics might also bind to hydrophobic sites in membrane proteins, but we do not think that anaesthetics work only by binding to membrane proteins. First of all because this would require the membrane proteins to have an immense amount of different binding sites for the different anaesthetics, and second of all because it would be peculiar if two so different substances as octanol and halothane would have so similar effects as our experiments show.

## 5.1  Outlook

T. Heimburg and A. Jackson argue [23] that a change in compressibility in the melting transition can lead to the possibility that solitons propagate in membranes, thereby causing nerve pulses. We have shown that the compressibility change in the phase transition of the lipid bilayer is lowered when anaesthetics are added to an artificial membrane. This result can be transferred to biological membranes [19], so the lowered compressibility change of the membrane could lead to a weakened nerve pulse. Furthermore anaesthetics lower the melting transition which makes it more difficult to get into the transition. As it according to [23] is necessary to push through the transition to get a nerve signal, this shift in melting temperature also could inhibit nerve pulses.

For further studies it could be interesting to make an AFM scan with octanol to see if domain size decreases, and a calorimetric scan with lipids containing a high concentration of diethylether, for example 100 w%, in order to see if this would yield an effect.

# 6   Acknowledgments

# Bibliography

[1] M. K. Jain (1988): *Introduction to Biological Membranes.* Wiley, New York

[2] S. J. Singer and G. L. Nicolson (1972): *The Fluid Mosaic Model of the Structure of Cell Membranes.* Science 1975: 720-731

[3] V. P. Ivanova (2000): *Theoretical and experimental study of protein-lipid interactions.* Ph.d. Thesis. Georg-August-Universität zu Göttingen.

[4] A. Hac (2003): *Diffusion Processes in Membranes Containing Coexisting Domains Investigated by Fluorescence Correlation Spectroscopy* Ph.d. Thesis. Georg-August-Universität zu Göttingen.

[5] T. Heimburg (2000): *A Model for the Lipid Pretransition: Coupling of Ripple Formation with the Chain-Melting Transtion* Biophys. J. 78: 1154-1165.

[6] H. M. Seeger, M. Fidorra and T. Heimburg (2005): *Domain Size and Fluctuations at Domain Interfaces in Lipid Mixtures.* Macromol. Symp. 219: 85-96.

[7] H. H. Meyer (1901): *Zur Theorie der Alkoholnarkose. Erste Mittheilung. Welche Eigenschaft der anästhetica bedingt ihre narkotische Wirkung?* Arhciv für experimentelle Pathologie und Pharmakologie 46: 338-346.

[8] C. E. Overton (1901): *Studien über die Narkose zugleich ein Beitrag zur allgemeinen Pharmakologie.* Gustav Fischer, Jena, Switzerland.

[9] J. G. Bovill (2000): *Mechanisms of anaesthesia: time to say farewell to the Meyer-Overton rule.* Anaesthesiology 13: 433-436.

[10] N. P. Franks and W. R. Lieb (1994): *Molecular and cellular mechanisms of general anaesthesia.* Nature 367: 607-614.

[11] M. D. Krasowski and N. L. Harrison (1999): *General anaesthetic actions on ligand-gated ion channels.* Cell. Mol. Life Sci. 55: 1278-1303

[12] R. S. Cantor (2001): *Breaking the Meyer-Overton Rule: Predicted Effects of Varying Stiffness and Interfacial Activity on the Intrinsic Potency of Anesthetics.* Biophys. J. 80: 2284-2297.

[13] R. S. Cantor (1999): *Lipid Composition and the Lateral Pressure Profile in Bilayers.* Biophys. J. 76: 2625-2639.

[14] R. S. Cantor (1999): *Solute Modulation of Conformational Equilibria in Intrinsic Membrane Proteins: Apparent "'Cooperativity"' without Binding.* Biophys. J. 77: 2643-2647.

[15] J. R. Trudell (1977): *A Unitary Theory of Anesthesia Based on Lateral Phase Separations in Nerve Membranes.* Anesthesiology 46: 5-10.

[16] M. Pickholz, L. Saiz and M. L. Klein (2005): *Concentration Effects of Volatile Anesthetics on the Properties of Model Membranes: A Coarse-Grain Approach.* Biophys. J. 88: 1524-1534.

[17] D. Pollakowski (2004): *Thermodynamische und strukturelle Untersuchungen an künstlichen und biologischen Membranen: Grundlegende Eigenschaften und der Einfluss kleiner Moleküle.* Master Thesis. Physics Deptartment, Univ. Göttingen.

[18] C. Kittel and H. Kroemer (2003): *Thermal Physics.* Second edition, Freeman.

[19] H. Ebel, P. Grabitz, T. Heimburg (2001): *Enthalpy and Volume Changes in Lipid Membranes. I. The Proportionality of Heat and Volume Changes in the Lipid Melting Transition and Its Implication for the Elastic Constants.* J. Phys. Chem. B 105: 7353-7360

[20] www.wikipedia.org/wiki/Atomic_force_microscope

[21] D. Glick: *Thermodynamic Flow Methods in Biochemistry.* Methods of Biochemical Analysis: 246-251, Wiley.

[22] H. J. Little and D. L. Thomas (1986): *The effects of anaesthetics and high pressure on the responeses of the rat superior cervical ganglion in vitro.* J. Physiol 374: 387-399.

[23] T. Heimburg and A. D. Jackson (2005): *On Soliton Propagating in Biomembranes of Nerves.* Proceedings of the Natural Academy of Sciences, USA. In press.